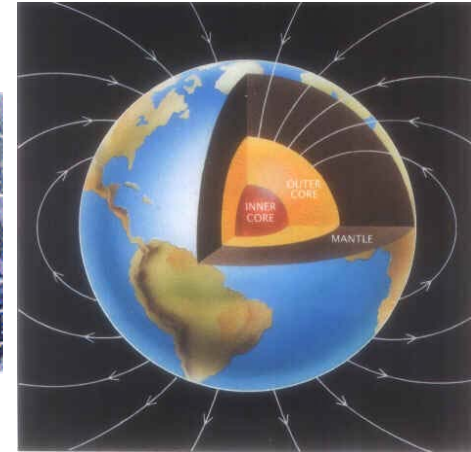
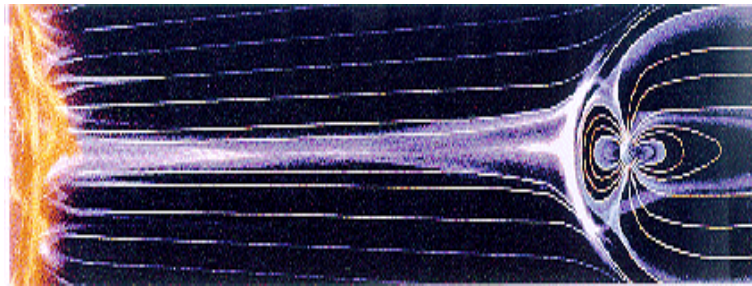
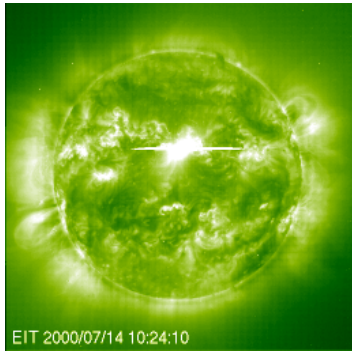


# Ground-based Instrumentation for Space Weather Observations II



Lectures for the ICTP School  
Trieste, Italy October 2010  
Peter Stauning, DMI



# Agenda:

## Introduction

### 4. Ionospheric radiowave propagation

4.1. Refractive index

4.2. Absorption

4.3. Scatter processes

### 5. Instrumentation for ionospheric observations

5.1. Ionosonde

5.2. Digisonde

5.3. GPS TEC

5.4. Riometers

5.5. Coherent scatter radar

### **6. Concluding remarks**

### **Links and references**

# Introduction

It is necessary to have an at least cursory insight in ionospheric physics and the propagation of radiowaves in an ionized medium in order to retrieve useful information from ionospheric data and understand how Space Weather conditions affect the various sounding methods.

So first a few basic relations.

# Ionospheric refraction

Electromagnetic waves propagating in an ionized medium are refracted, reflected, absorbed, and scattered. Some of these processes can be described in relatively simple terms:

The harmonic wave electric field,  $\mathbf{E}$ , is assumed to create polarisation,  $\mathbf{P}$ , in the medium by displacing electrons and ions differently.

The resulting displacement vector,  $\mathbf{D}$ , is then:

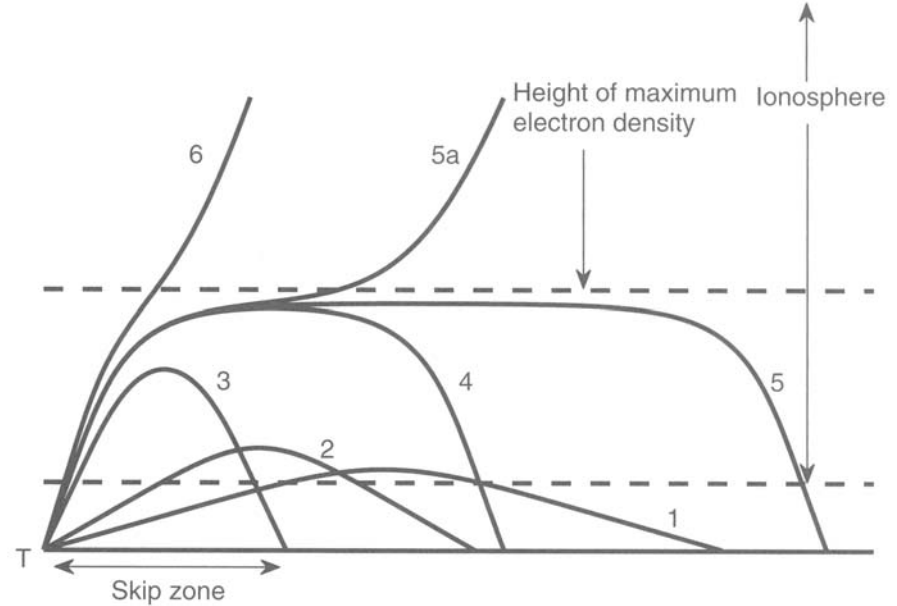
$$\mathbf{D} = \epsilon_0 \mathbf{E} + \mathbf{P} = \epsilon \mathbf{E}$$

The phase speed of the wave is:

$$v_{\text{ph}} = 1/(\epsilon\mu_0)^{1/2}$$

and the refractive index is:

$$n^2 = (c/v_{\text{ph}})^2 = \epsilon/\epsilon_0 = 1 + \mathbf{P}/(\epsilon_0 \mathbf{E})$$



[Levis et al. (2010), p.265]

Fundamentally, the issue is reduced to solving the equations of motion for electrons and ions in a harmonic wave field (usually the wave magnetic field can be neglected) and inserting the solution in the wave equation to solve for the (generally complex) refractive index  $n$ .

## Ionospheric refraction. No magnetic field.

For a medium with free electrons and no external magnetic field, the electron equation of motion in the harmonic wave field,  $\exp(i(\omega t - kx))$ , takes the form:

$$m_e \frac{d^2x}{dt^2} = q E - m_e \nu \frac{dx}{dt} \quad \rightarrow \quad -m_e \omega^2 x = q E - m_e \nu i \omega x$$

where  $x$  denotes the transverse electron motion,  $m_e$  the electron mass,  $q$  is the electron charge, and  $\nu$  its effective collision frequency.

Solving for the polarization,  $P = q N_e x$ , gives:

$$P = -N_e q^2 E / (m_e \omega^2 - m_e \nu i \omega)$$

Introducing now the plasma frequency  $\omega_p^2 = N_e q^2 / \epsilon_0 m_e$ , and the dimensionless quantities  $X = \omega_p^2 / \omega^2$  and  $Z = \nu / \omega$  gives for the refractive index:

$$n^2 = (\mu - i\chi)^2 = 1 - X / (1 - iZ) = 1 + X Z / (1 + Z^2) - i X Z / (1 + Z^2)$$

where the refractive index is now divided in a real part,  $\mu$ , and an imaginary part,  $\chi$ . The real part is primarily responsible for the changes in the wave phase and group velocities while the imaginary part is related to the collisional damping of the wave.

Note that the refractive index is zero when  $X = 1$ . The phase velocity goes to infinity and the group velocity goes to zero. If the wave is entering a medium with gradually increasing electron density (i.e., increasing plasma frequency) then the wave is totally reflected at the level where  $X = 1$ .

## Ionospheric refraction

Turning now to the real ionosphere with a stationary magnetic field,  $\mathbf{B}$ , and introducing the dimensionless quantities  $Y = \omega_b/\omega$ ,  $Y_L = Y\cos\theta$ , and  $Y_T = Y\sin\theta$ , where  $\omega_b$  is the gyro frequency ( $=qB/m_e$ ), while  $\theta$  is the angle between the stationary magnetic field and the propagation direction. In the electron equation of motion solving for the polarisation in the medium, two solutions for the wave polarisation appear :

$$R = \frac{i}{2Y_L} \left\{ \frac{Y_T^2}{(1-X-iZ)} \mp \sqrt{\frac{Y_T^4}{(1-X-iZ)^2} + 4Y_L^2} \right\}$$

which, when used in the wave equation to derive the refractive index, gives the Appleton-Hartree formula:

$$n^2 = 1 - \frac{X}{1-iZ - \frac{Y_T^2}{2(1-X-iZ)} \pm \sqrt{\frac{Y_T^4}{4(1-X-iZ)^2} + Y_L^2}}$$

when collisions are neglected ( $Z = 0$ ) it has the simpler, real form:

$$\mu^2 = 1 - \frac{2X(1-X)}{2(1-X) - Y_T^2 \pm \sqrt{Y_T^4 + 4(1-X)^2 Y_L^2}}$$

The refractive index has zeros (total reflection) for the following conditions:

- With + sign:  $X = 1$  (ordinary wave: "O")
- With - sign:  $X = 1-Y$  (extraordinary wave: "X")
- $X = 1+Y$  (extraordinary wave: "Z")

## Ionospheric absorption

Electromagnetic (radio-) waves passing through an ionized medium are absorbed when the electrons, set in motion in the wave field, are disturbed by collisions and thus prevented from re-radiating the accumulated wave energy. The absorption may be derived from the general formula for the complex refractive index. Using for the refractive index the simple formula that neglects the magnetic field gives for the complex refractive index:

$$n^2 = (\mu - i\chi)^2 = 1 - \frac{X}{1 - iZ} = 1 - \frac{X}{1 + Z^2} - \frac{iXZ}{1 + Z^2}$$

For a wave travelling in the  $x_1$  direction the wave field can be written as the product of an infinite plane wave and an exponentially decaying factor:

$$E = E_0 \exp\left(-\chi \frac{\omega}{c} x_1\right) \exp i\left(\omega t - \frac{\omega}{c} \mu x_1\right)$$

The decay of amplitude in unit distance is called the absorption coefficient,  $\kappa = \chi\omega/c$  and is now found by equating the imaginary terms of the above expression for the refractive index and inserting the parameters for X and Z:

$$\kappa = \frac{\omega}{c} \frac{1}{2\mu} \frac{XZ}{1 + Z^2} = \frac{e^2}{2\epsilon_0 m c} \frac{1}{\mu} \frac{N\nu}{\omega^2 + \nu^2}$$

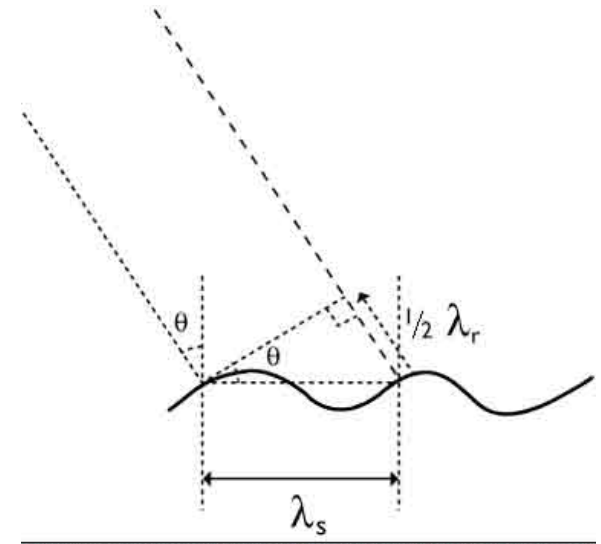
Usually, the collision frequencies are much smaller than the wave frequencies of interest for transmission services (i.e.,  $\nu \ll \omega$ ). Hence absorption processes are particularly important either when the collision frequencies,  $\nu$ , are large even when the electron densities,  $N$ , are rather low such that the refractive index,  $\mu$ , is near unity (non-deviative absorption) or for moderate collision frequencies when the electron densities are large enough to cause the refractive index to approach zero (deviative absorption).

## Ionospheric scatter processes

For an incoming wave at wavelength  $\lambda_s$  that is affected by a structure with irregularities repeated at distances  $\lambda_s$  and extended in the perpendicular direction, then the backscattered signals at an angle  $\theta$  from the individual scatters are all in phase if the Bragg condition is fulfilled:

$$n \lambda_r = 2 \lambda_s \sin \theta$$

where  $n$  is an integer. It should be noted that the incoming wave must arrive in directions perpendicular to the elongation of the structure



Wave-like ionospheric structures can be generated by plasma instability processes, for instance, by strong electric fields that make the electrons move fast relative to the ions in regions (notably the E-region) where the collisions tend to stop the ion motion (two-stream instability), or by strong density gradients (gradient-drift instability) in drifting ionosphere regions (E- and F- regions).

But such periodic structures could also be impressed from outside conditions like turbulence in the upper atmosphere associated with tides and gravity waves in the lower regions (D- and E-regions) or by impinging large-scale waves or modulated electron precipitation initially generated in the magnetosphere.

It should be mentioned that the coupled thermal motion of electrons and ions can be resolved into a spectrum of ion-acoustic plasma waves.

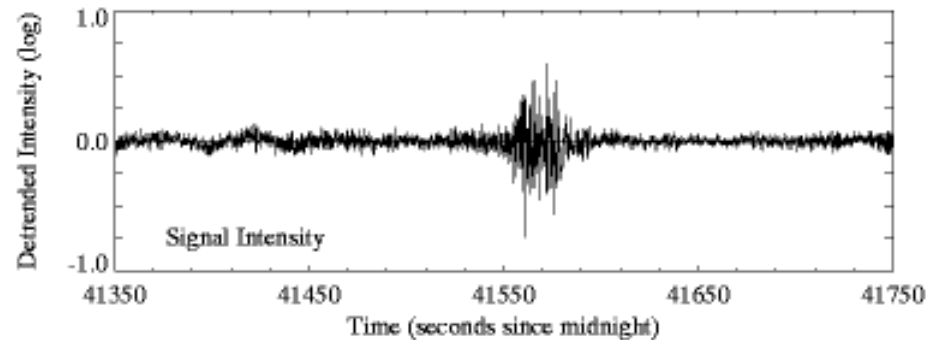
## Ionospheric scatter processes

These scatter processes give rise to a host of radio wave phenomena. For ionosonde or digisonde observations they cause backscatter reflections that may give additional traces from sporadic layers (e.g., E<sub>ss</sub>) or massive spread reflections over wide height and frequency ranges (e.g., spread-F) that in turn may blur large sections of the ionograms.

For coherent scatter techniques like that used in the STARE or Super DARN radar systems, the ionospheric scatter of the radar signals is a prerequisite for the measurements. For these observations the transmitted rays need to enter perpendicular to the magnetic field direction to fulfil the backscatter conditions.

For the “incoherent” radars (which are not quite incoherent), the major backscatter process is the coherent Bragg-scattering from ion-acoustic structures generated by the thermal motions.

For signals propagated through ionospheric regions with scatter activity the amplitudes and phases of the received waves may fluctuate strongly, which give rise to so-called scintillations in the received signal as illustrated

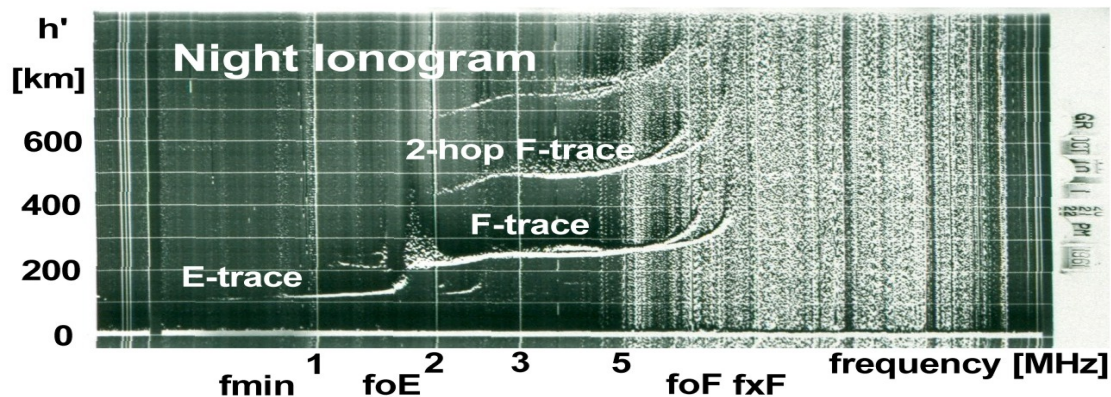


[[http://www.nwra.com/ionoscint/sp\\_intro.html](http://www.nwra.com/ionoscint/sp_intro.html)]

# Ionosondes

The ionosonde is essentially a swept frequency radar that measures the elapsed time between the transmission of continuous wave (CW) pulses and the reception of their reflections from the ionosphere. Assuming propagation at the speed of light,  $c$ , the delay,  $\Delta t$ , measures the virtual (apparent) height of the reflecting layer:  $h' = 0.5c \Delta t$ . The real height is lower since the true signal (group) velocity is always lower than  $c$ .

The signal can be used to blank the trace (B-scan). If the screen is photographed on a slowly moving film then an ionogram picture is formed in the course of the frequency sweep. The trace from a pulse corresponds to a vertical line in the ionogram. The base-line (0 km) mark the transmission.



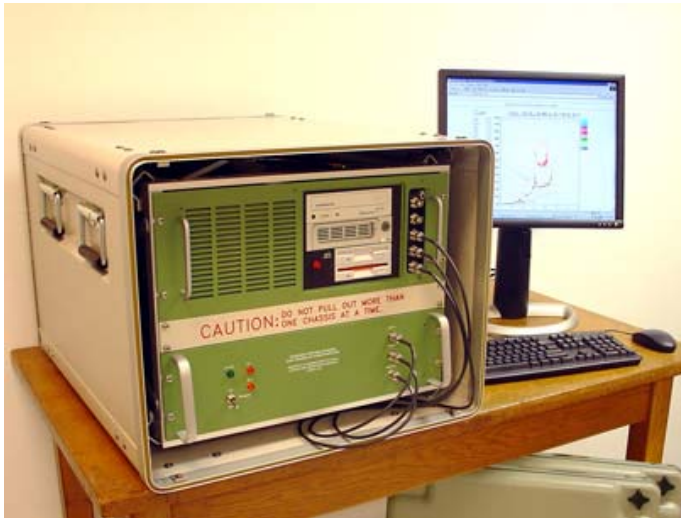
Ionosonde formerly installed in Narsarsuaq, Greenland.



[Photos: DMI]

# Digisondes

Now, most (analog) ionosondes have been replaced by digisondes. The operating principle of a digisonde resembles that of the ionosonde. A widely used instrument is the University of Lowell “Digisonde Portable Sounder” (DPS). [<http://ulcar.uml.edu/DPS.htm>].



Upper left: Univ. Lowell Digisonde. Lower left: Receiver antenna. Above. Digisonde installation in Narsarsuaq. Note the tower that carries the transmitting delta antenna.

[Photos: DMI]

# Digisondes

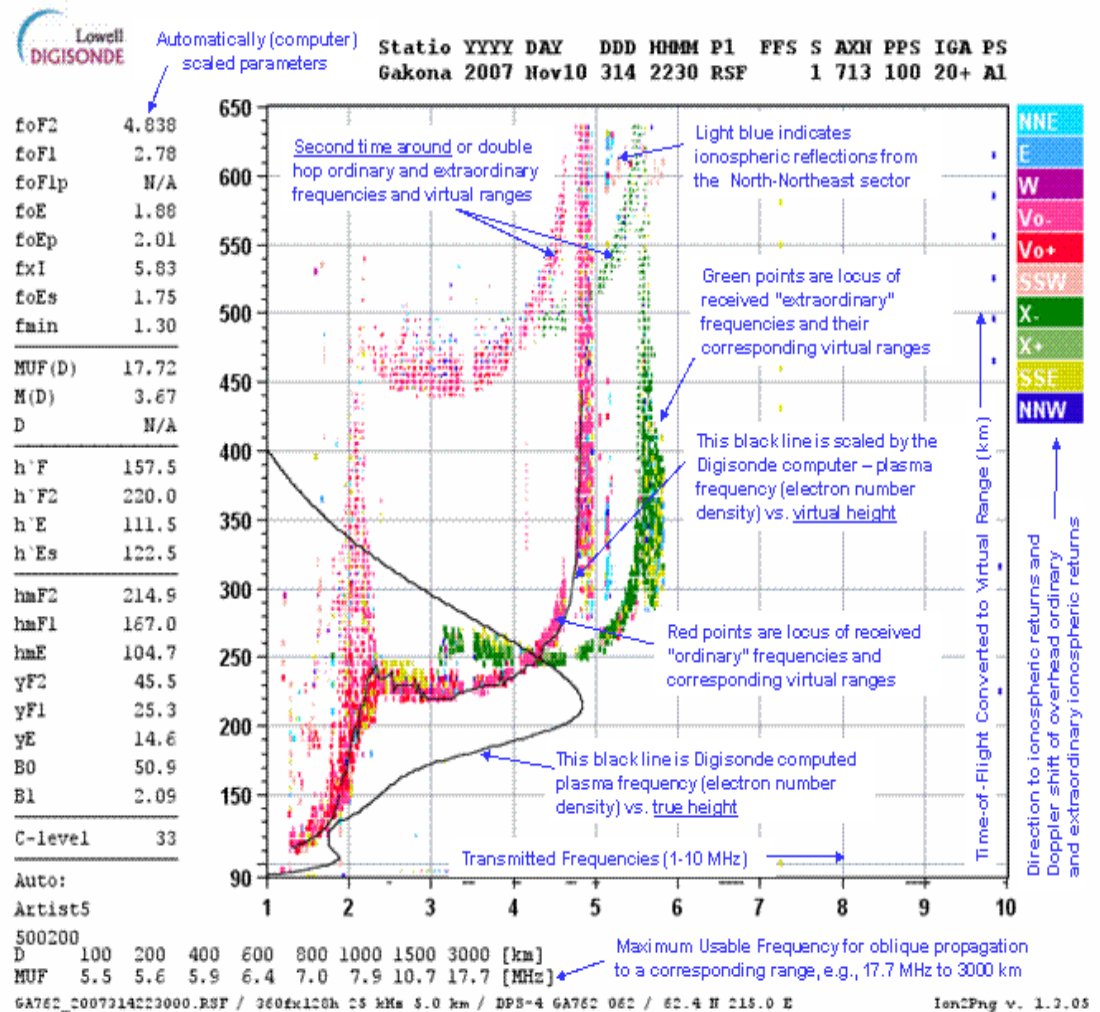
The University of Lowell Digisonde instrument performs simultaneous measurement of seven observable parameters of reflected (or in oblique incidence, refracted) signals received from the ionosphere:

- 1) Frequency
- 2) Range (or height for vertical incidence measurements)
- 3) Amplitude
- 4) Phase
- 5) Doppler Shift and Spread
- 6) Angle of Arrival
- 7) Wave Polarization

Ordinary reflection:  $f = f_p$

Extraord. reflection:  $f = f_p + \frac{1}{2}f_p$

Electron density:  $N_e = f_p^2 / 80.5$



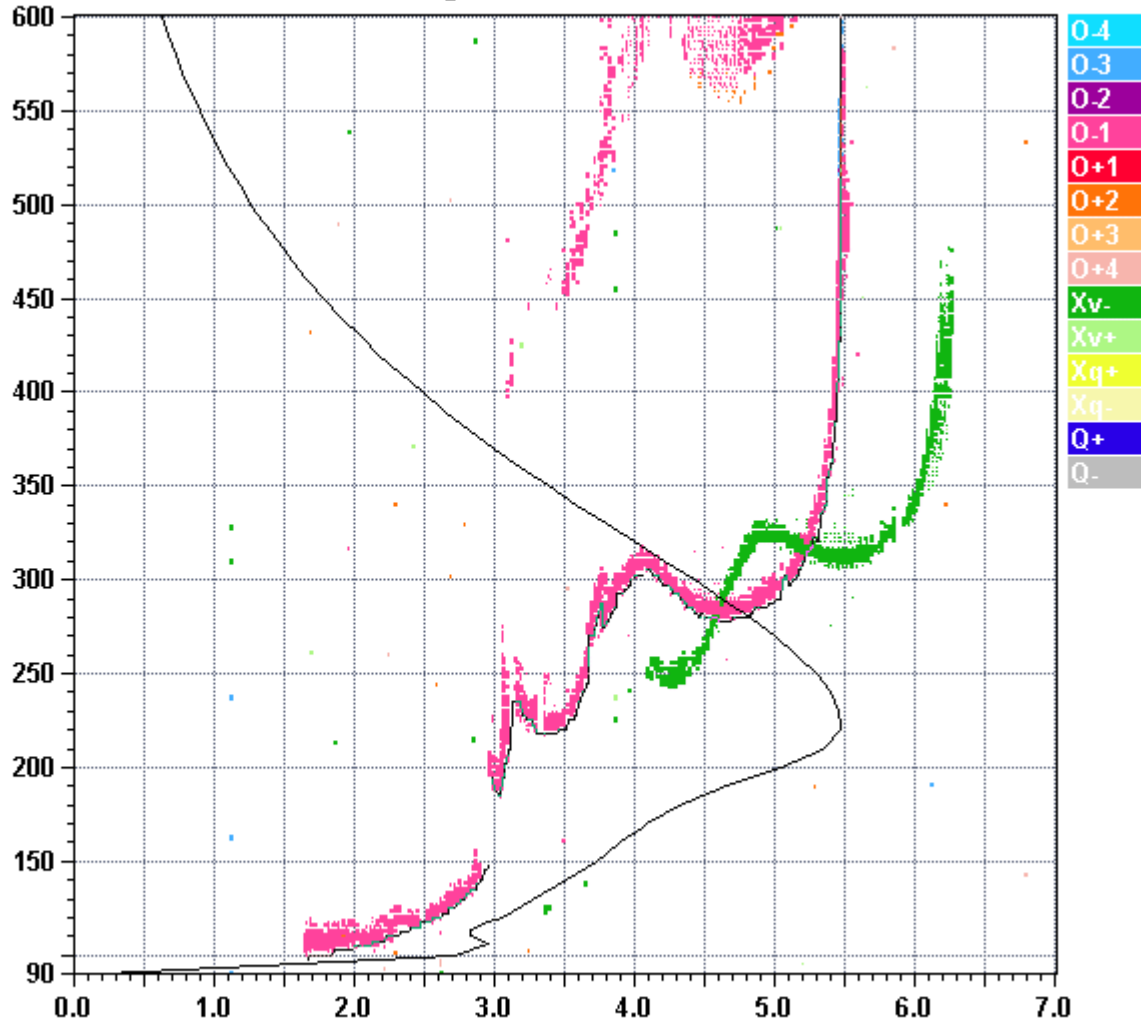
[<http://ulcar.uml.edu/DPS.htm>]

# Digisondes



Station Millstone Hill 1996 Apr01 092 1934 SBF FFS S AXN PPS IGA PS  
 1 015 100 00+ B0

foF2	5.481
foF1	4.05
foF1p	4.02
foE	2.96
foEp	2.91
fxI	6.20
foEs	2.95
fmin	1.65
<hr/>	
MUF(D)	18.70
M(D)	3.42
D	3000.0
<hr/>	
h`F	185.0
h`F2	277.5
h`E	97.5
h`Es	98.8
<hr/>	
hmF2	223.1
hmF1	168.4
hmE	106.3
yF2	60.0
yF1	48.4
yE	16.0
B0	79.3
B1	1.74
<hr/>	
C-level	N/A



D 100 200 400 600 800 1000 1500 3000 [km]  
 MUF 6.2 6.2 6.5 7.0 7.7 8.6 11.4 18.7 [MHz]

6092T34H.SBF / 280fx512h 25 kHz 2.5 km / DPS-1 MHJ45 042 / 42.6 N 288.5 E

[<http://ulcar.uml.edu/DPS.htm>]

Ion2Png v. 1.1.02

# Ionograms: Sporadic layers

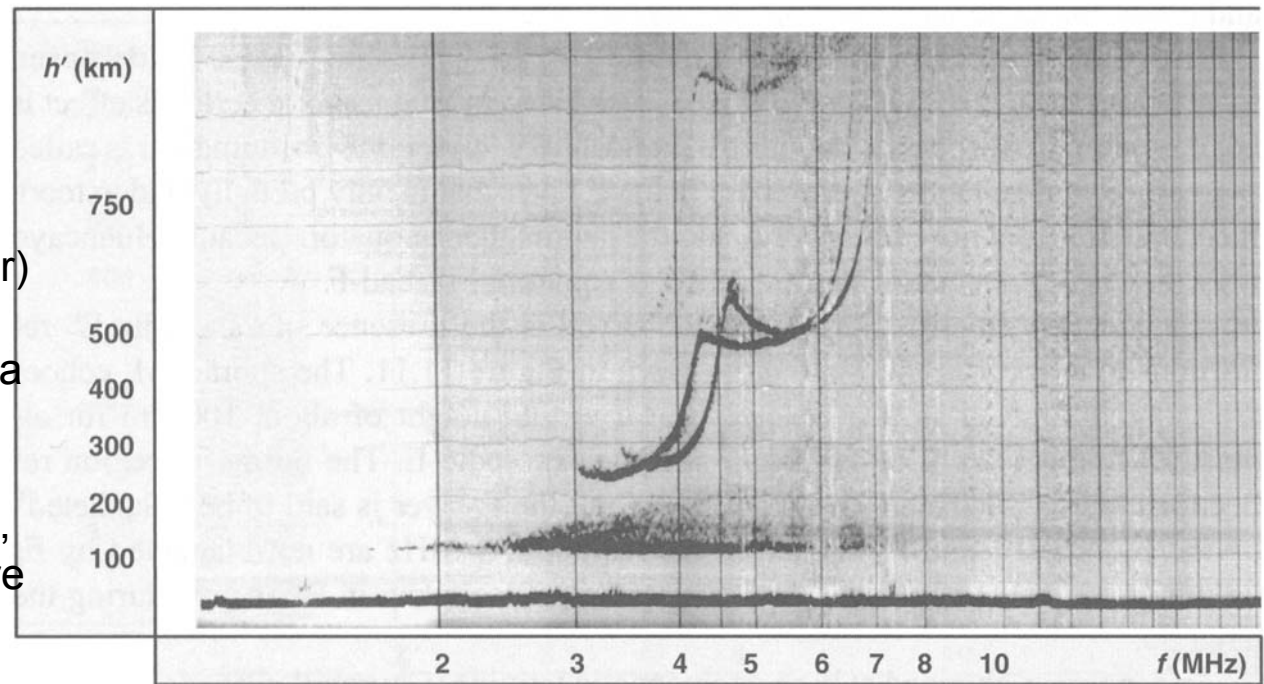
**Sporadic layers.** Additional ionization may be produced by various processes, among other, precipitation of energetic electrons during auroral substorm events. During such events that are most frequent at the night side of the auroral regions, intense showers of energetic particles, primarily electrons and protons, may enter the upper atmosphere. One of the consequences is the formation of strongly enhanced E-layers at altitudes of around 100-150 km.

## Es layers may:

- enhance the signal strength for short-range transmissions
- disabled long-range transmission (via F-layer) by the shielding (“blanketing”) effects of a dense E-region

In most cases, however, the sporadic E-layers are partly transparent such that signals can pass

through to reach F-region altitudes. An example is presented above.

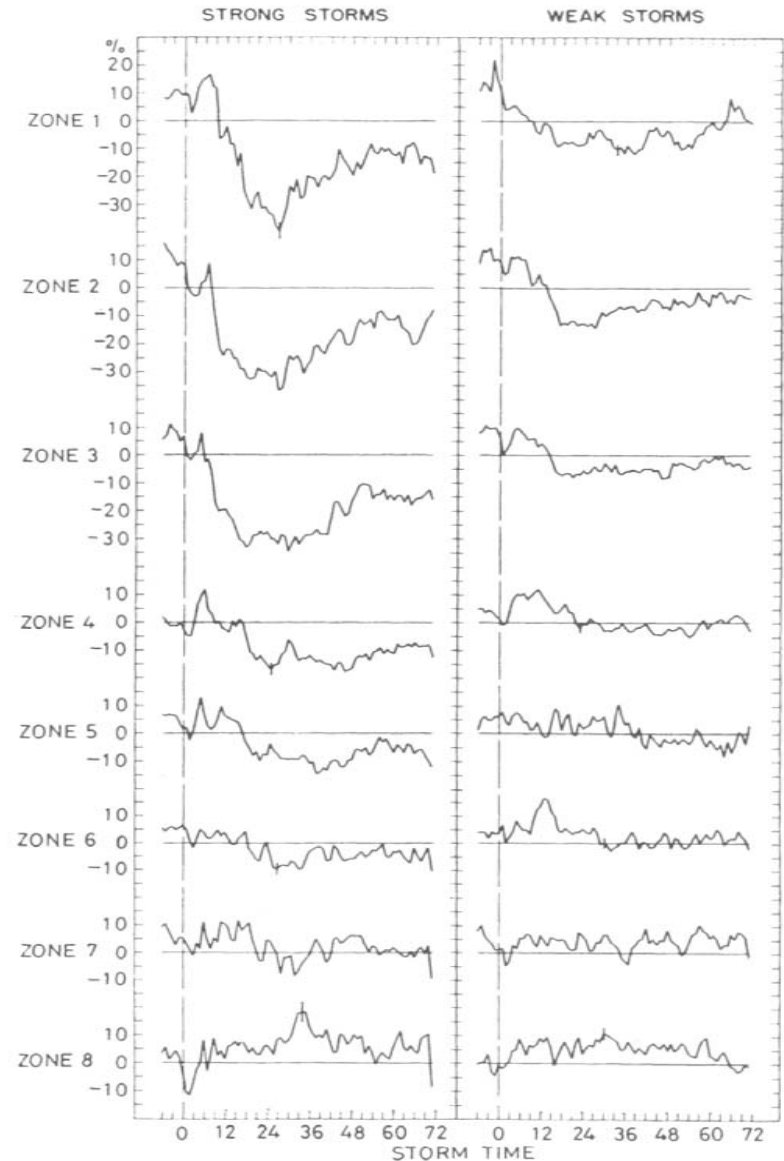
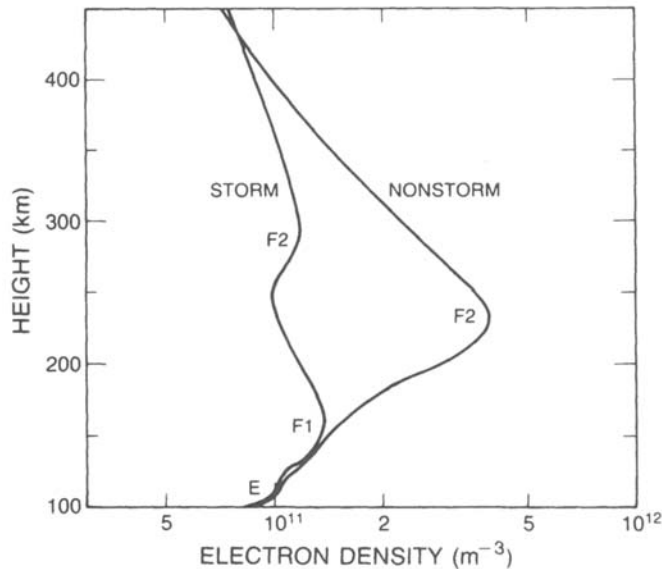


[Levis et al. (2010), p.256]

# Ionograms: F-region depression

During magnetic storms the F-region electron densities, and thus the max frequencies for reflections, can be dramatically reduced (see examples).

At the same time absorption processes in the D-region may cause black-out at lower frequencies. These effects narrow (or close) the frequency range for communication.



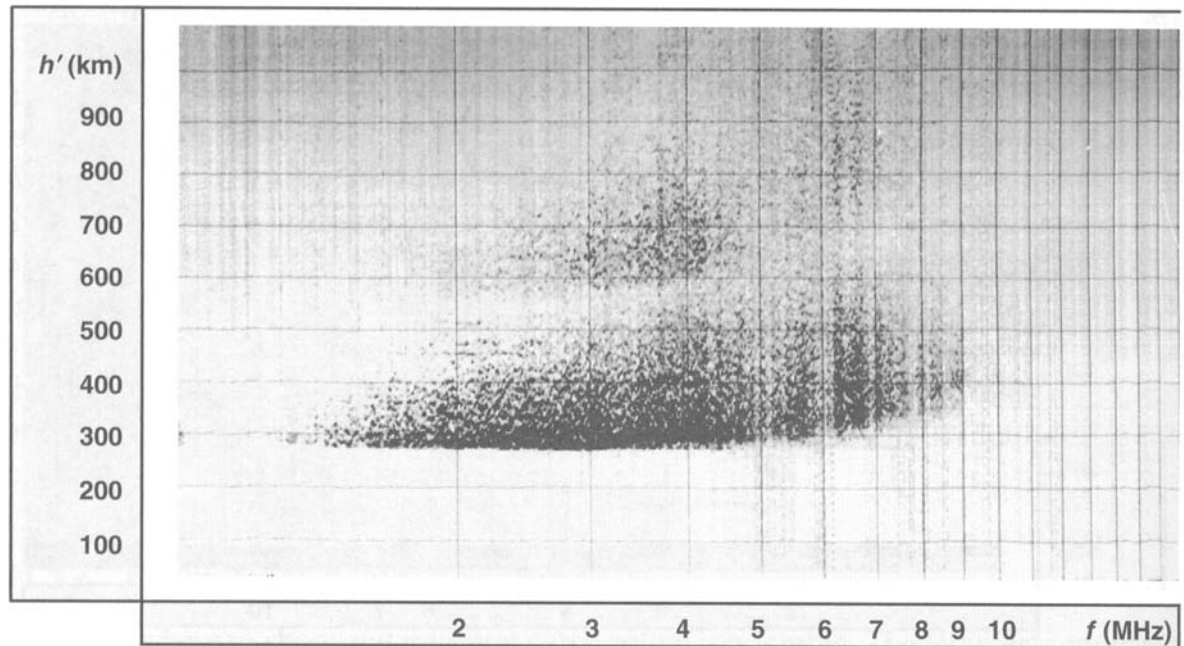
[Davies (1990), pp.339, 341]

# Ionograms: Backscatter

Various plasma processes may generate wave-like structures in the ionosphere. Such disturbances are in particular frequent at conditions that produce large ionospheric electric fields and currents related, for instance, to the auroral or equatorial electrojets.

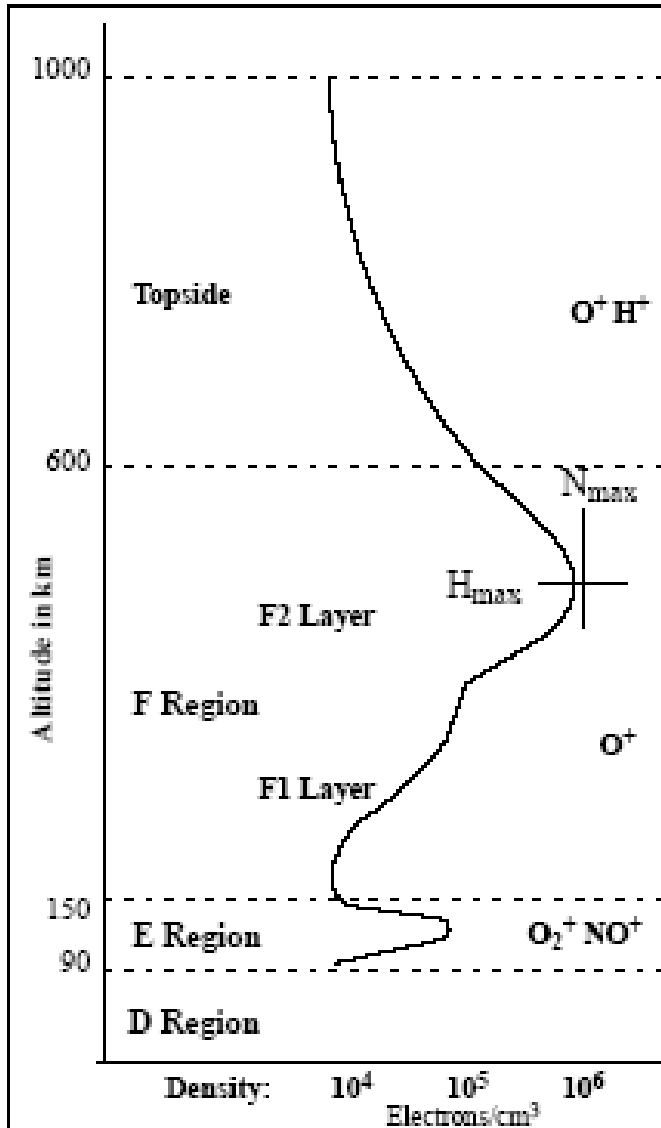
In the ionograms such conditions produce scattered return signals, i.e., backscatter, which may blur the regular reflections (see example).

Scatter can disturb the signals both by scattering power out of the transmitted radio signals and also by adding unwanted spurious contributions in and out of phase with the main signal and produce scintillations in the strength and phase of the received signal



[Levis et al. (2010), p.256]

# TOTAL ELECTRON CONTENT (TEC)

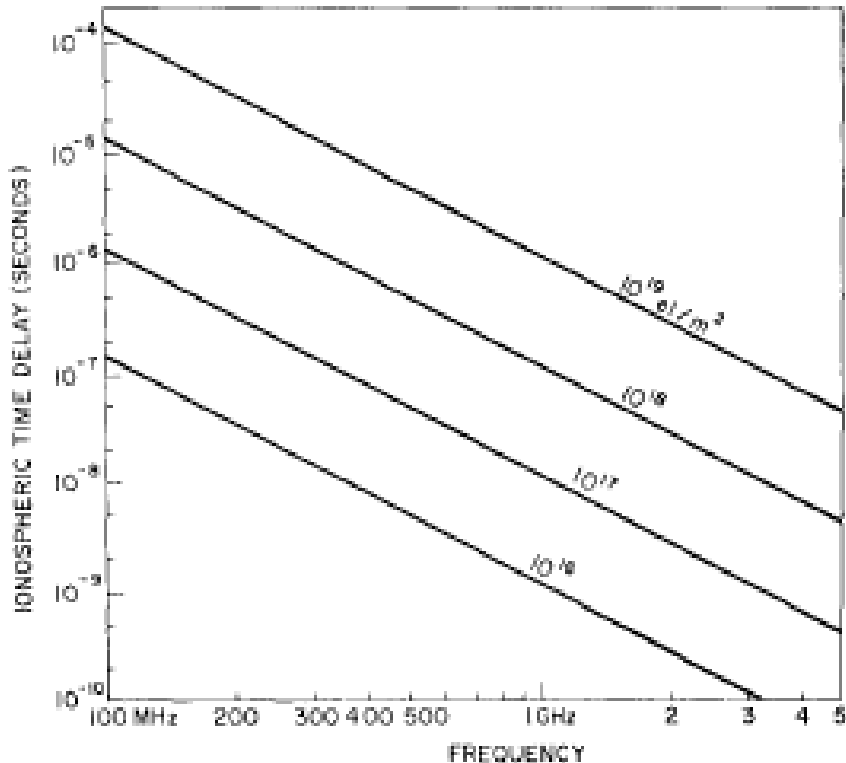


The figure displays a typical ionospheric electron density profile. The profile continues smoothly upward with a generally decaying electron density.

Total electron content (TEC) is an important ionospheric parameter for navigation customers. All single-frequency GPS receivers (millions of users) must correct for the delay of the GPS signal as it propagates through the ionosphere from GPS satellites at 22,000 km altitude. TEC controls this delay and a correction is required if an accurate position location is to be provided by the GPS receiver.

[<http://www.swpc.noaa.gov/info/lono.pdf>]

# TOTAL ELECTRON CONTENT (TEC)



[Davies (1990), p.279]

## Ionospheric delay

The additional delay of a signal transmitted from above the ionosphere to a user on the Earth is:

$$\Delta t [\text{sec}] = (40.3/cf^2) \text{ TEC}$$

where TEC is the total number of electrons in a unit cross section column along the path,  $c$  the velocity of light, and  $f$  the system operating frequency.

Generally, TEC ranges from  $\sim 10^{17}$  to  $10^{18}$  [el/m<sup>2</sup>]

At the higher GPS frequency (1575 MHz) this delay corresponds to a distance of:

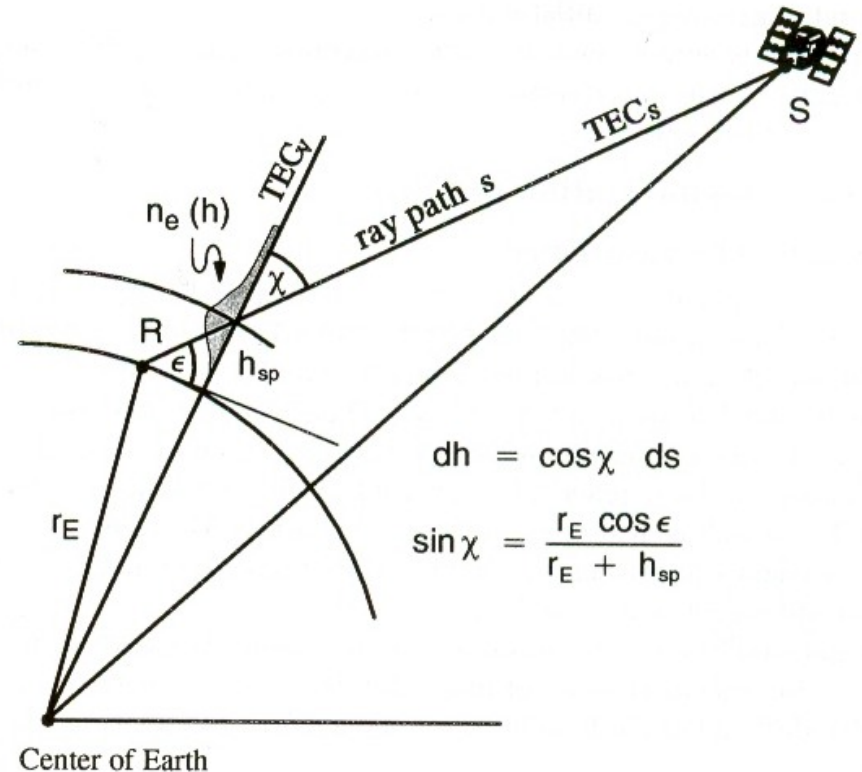
$$\Delta x = 0.16 \text{ m} * \text{TEC (in units of } 10^{16} \text{ el/m}^2)$$

# TOTAL ELECTRON CONTENT (TEC)

The ionospheric influence on radio signals can be described in terms of the refractive index, which differs from unity and, therefore, causes changes in amplitude, phase, polarization and ray path of radio waves propagating through the medium.

The corresponding effects on navigation signals comprise signal code propagation delays and advancements of signal carrier phase.

These effects, while degrading the accuracy of navigation signals, can however be used in the diagnostics of the ionosphere particularly in dual frequency (or dual polarization) measurements between a spacecraft and a ground station.



Satellite-ground transmissions.  
[Jacowski, 1996 (in Kohl, 1996, p373)]

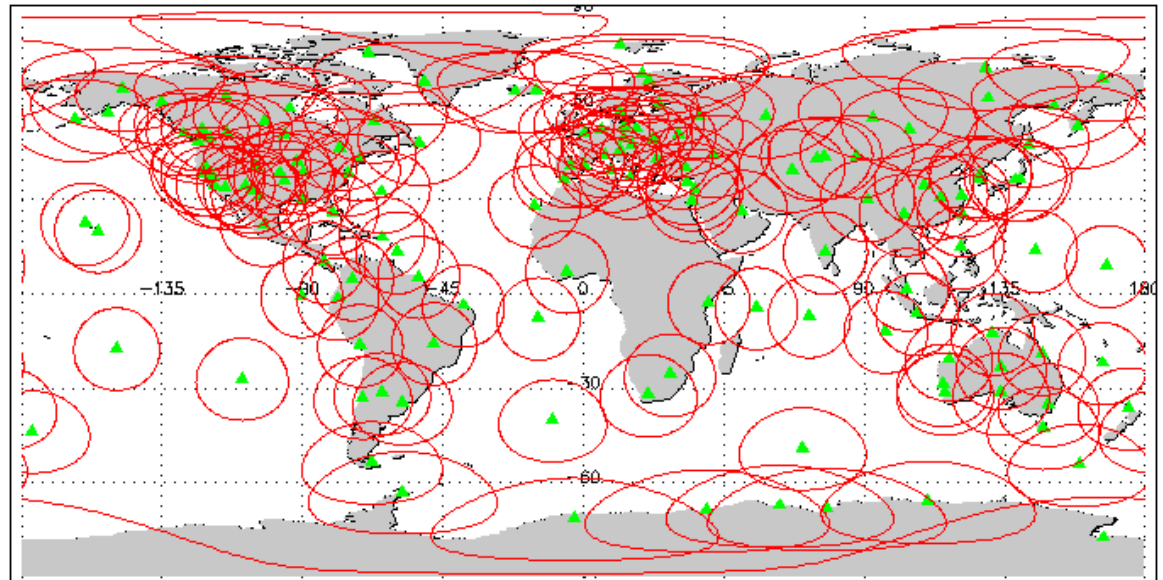
# TOTAL ELECTRON CONTENT (TEC)

The GPS satellites transmit two coherent frequencies in the L-band, at L1 with  $f_1=1575.42$  MHz and L2 with  $f_2=1227.60$  MHz. The L1 frequency is modulated by a public Coarse/Acquisition (C/A) code with an effective modulation frequency of around 1 MHz (wavelength~300m). Both carrier frequencies are modulated by a precise (P or Y) code with an effective modulation frequency of around 10 MHz (wavelength~30m). The ionospheric contribution to the difference in pseudo ranges (i.e. phase difference when down-converted to a common reference frequency) between L1 and L2 signals is:

$$\Delta p_l = p_2 - p_1 = K (1/f_1^2 - 1/f_2^2) \text{ TEC}$$

where  $K = 40.3 \text{ [m}^3/\text{s}^2]$

From such measurements the oblique TEC is obtained. Using a worldwide array of GPS receiving stations (map) enables the construction of global vertical TEC distributions (e.g. used in the “Global Assimilative Ionospheric Model”, GAIM).

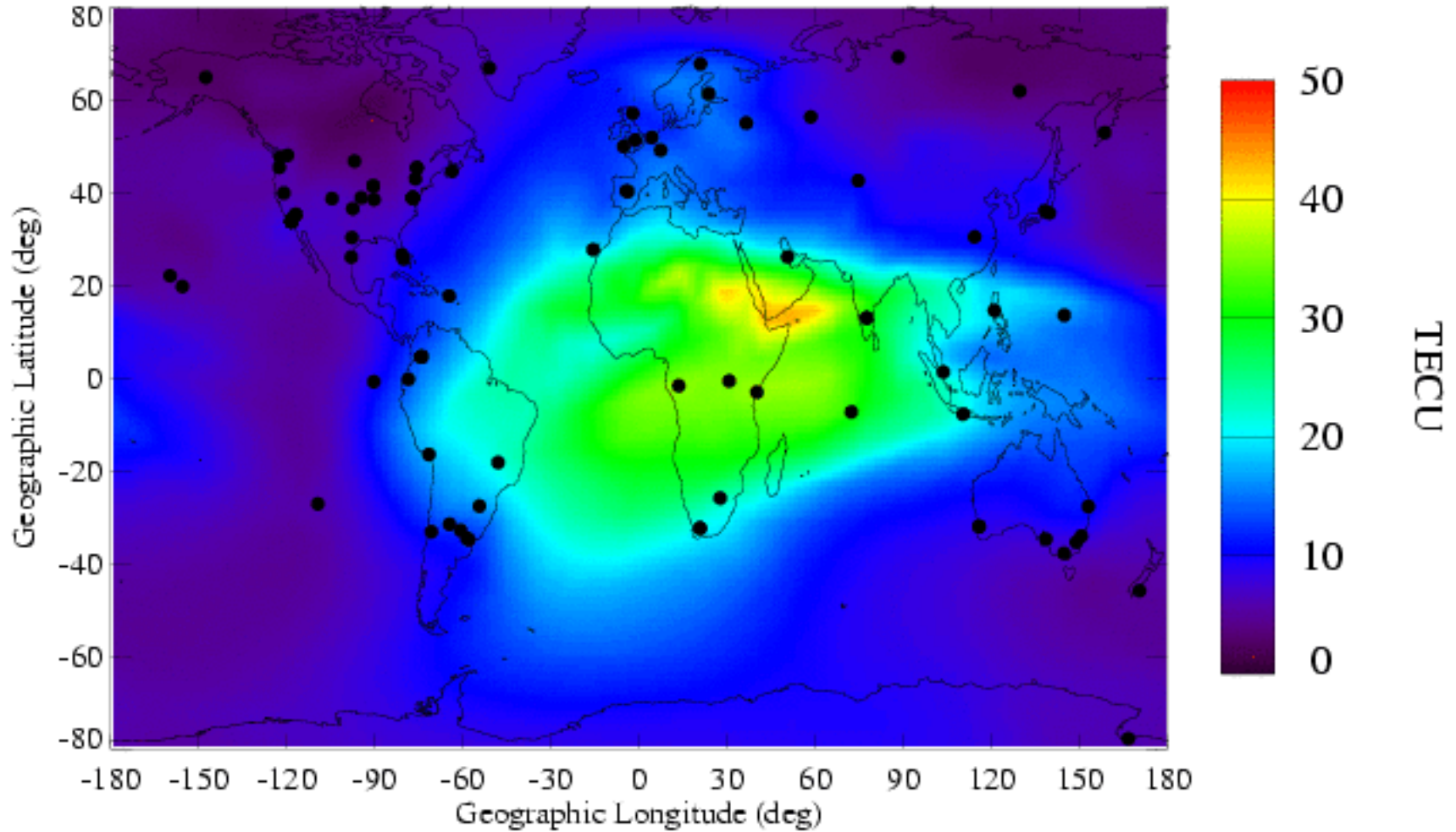


[<http://iono.jpl.nasa.gov/gaim/intro.html>]

# TOTAL ELECTRON CONTENT (TEC)

10/30/05  
12:20 UT

## Ionospheric TEC Map

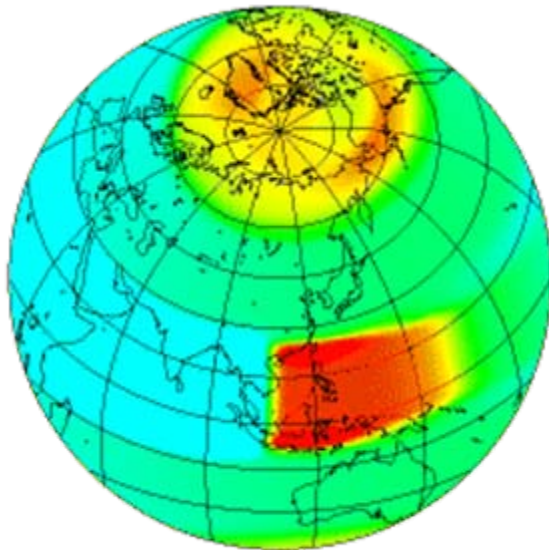


• GPS Receiver

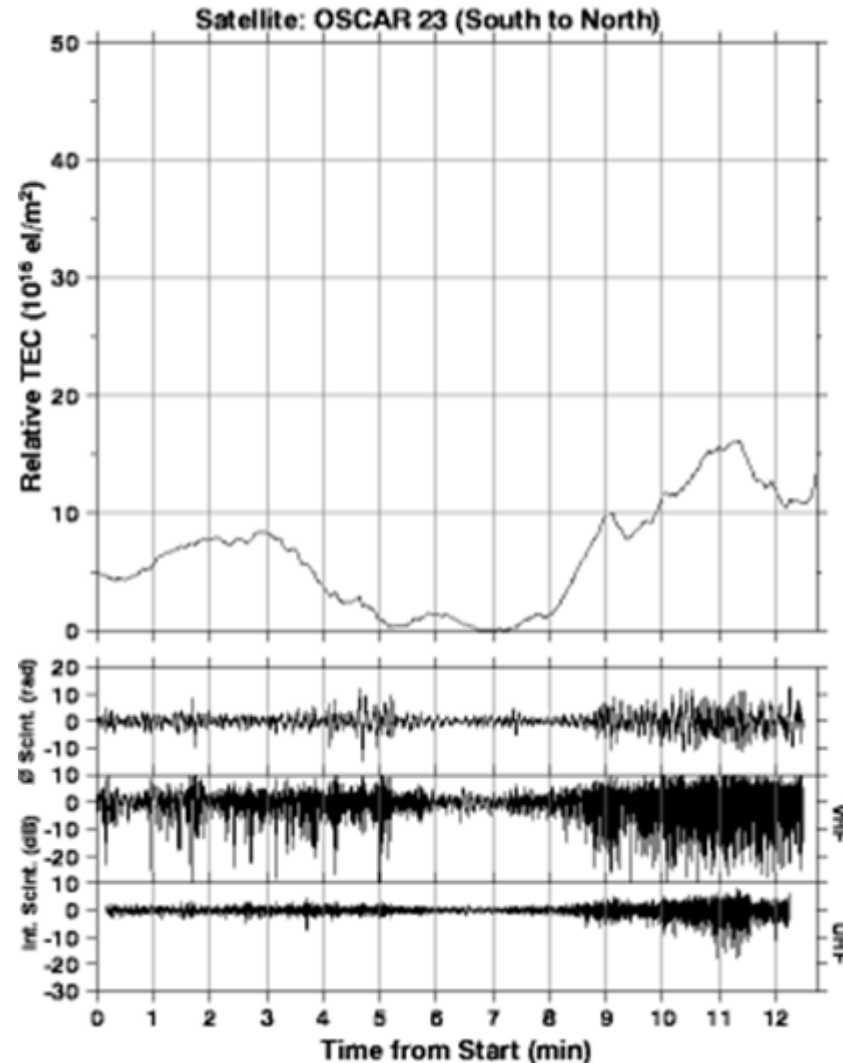
[Ref.: [iono.jpl.nasa.gov/latest\\_rti\\_global.html](http://iono.jpl.nasa.gov/latest_rti_global.html)]

# TEC and Ionospheric Scintillations

The reception of signal from satellite-borne transmitters enables the study of ionospheric scintillations. The right figure displays an example of TEC results and signal scintillations. Such scintillations are most frequent during magnetic storms and may degrade a.o. GPS reception. Below is shown an example of global scintillation occurrences.



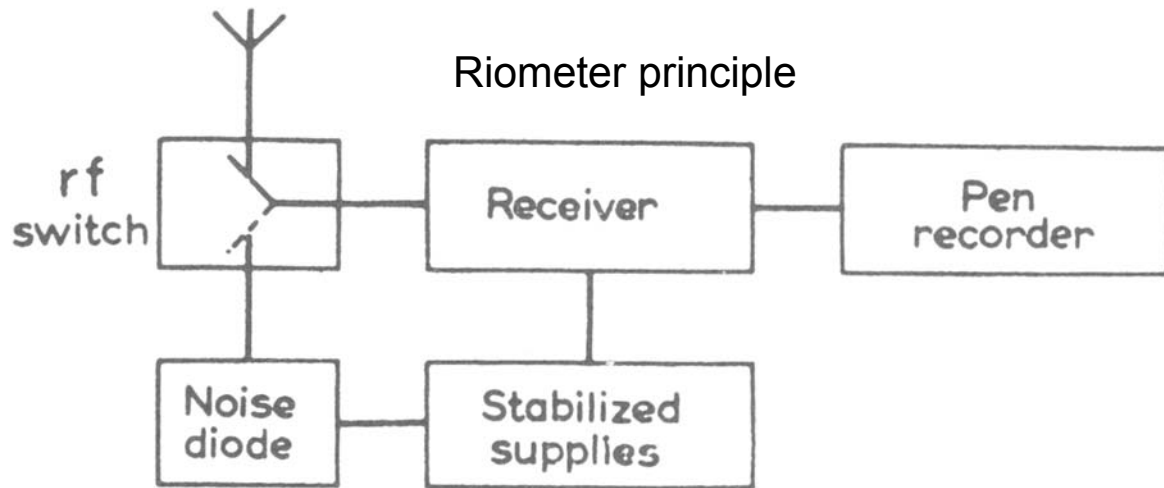
Copyright 1995, Northwest Research Associates, Inc.



[[http://www.nwra.com/ionoscint/sp\\_intro.html](http://www.nwra.com/ionoscint/sp_intro.html)] ]

# Riometers

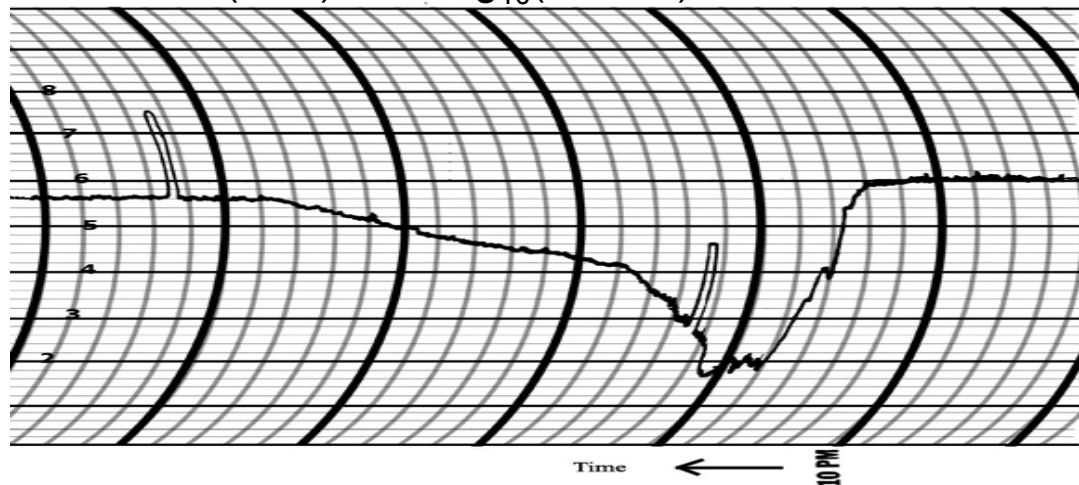
A RIOMeter (Relative Ionospheric Opacity - meter) is, in principle, a sensitive, calibrated radio receiver that measures the signal strength of the weak signals received from sources in the sky and thus repeated each sidereal day.



Most often a vertical antenna is being used for single-beam riometer observations. The measuring frequency is normally in the HF-VHF frequency range, typically around 30 MHz.

The riometer technique to measure ionospheric absorption was developed during the IGY years by Little and Leinbach (1959).

Chart recording with absorption event:  
 $A(\max) = 10 \log_{10}(0.6/0.2) = 4.8 \text{ dB}$



<--- Time

[<http://www.lajollasciences.com>]

# Single-beam Riometers

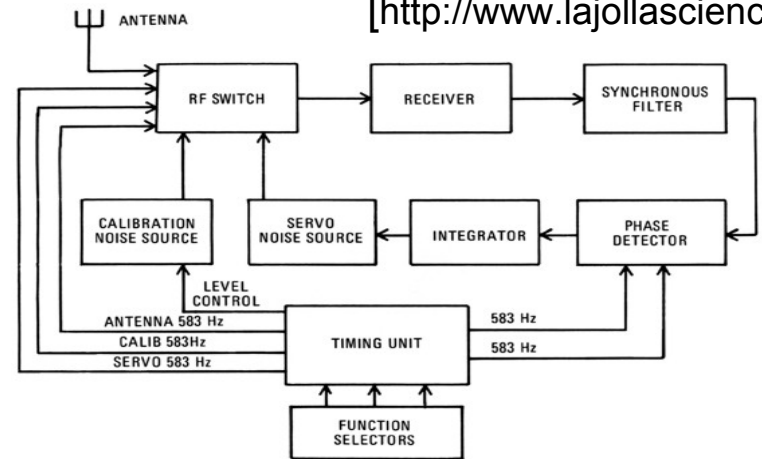
The upper figure displays a block diagram of a modern LaJolla riometer. The instrument has been manufactured for almost 40 years in continually updated versions.

The standard version uses a wide-beam double dipole antenna structure. However, more directive antenna systems are often desirable.

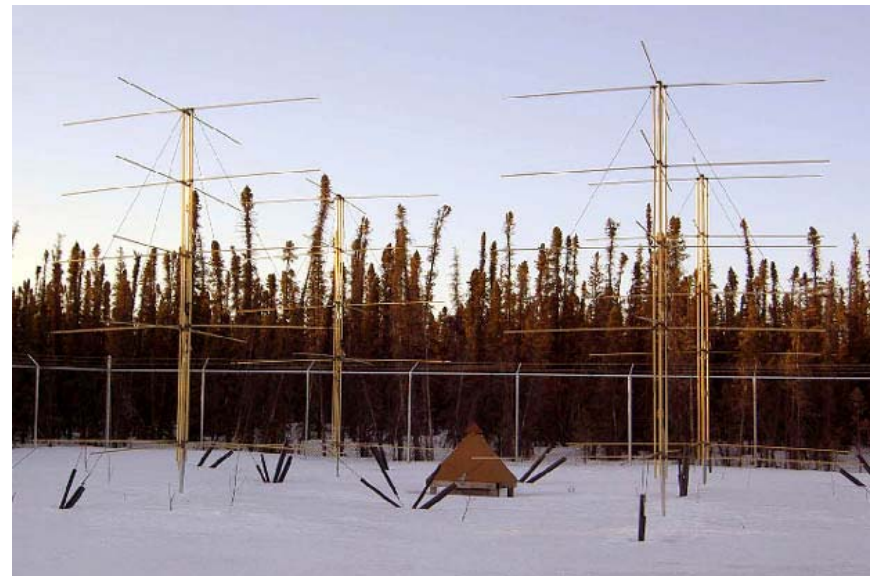
The lower figure displays the antenna system with 4 crossed Yagi antennas used for single-beam riometer observations at the HAARP research facility in Alaska.

[ <http://www.haarp.alaska.edu/haarp/data.html> ]

[<http://www.lajollasciences.com>]



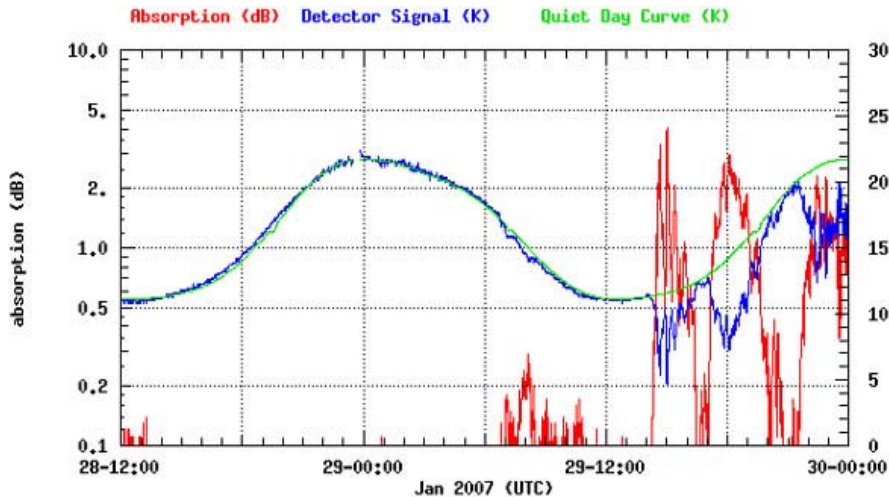
RIOMETER BLOCK DIAGRAM



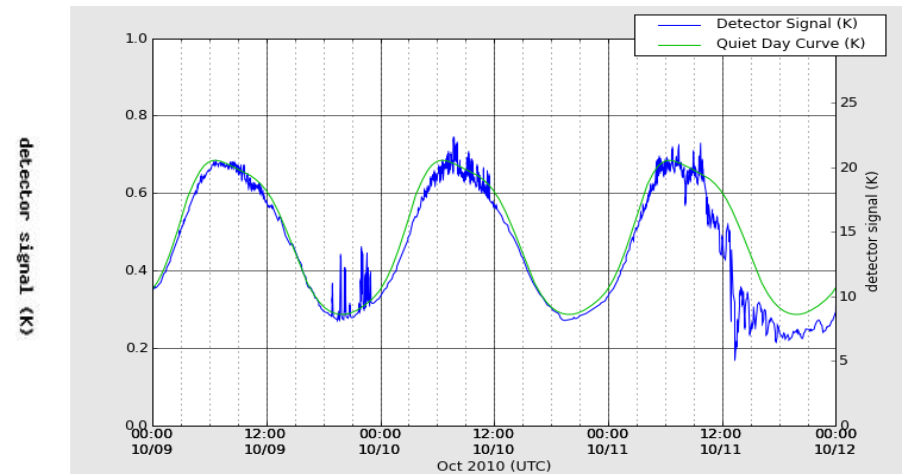
# Single-beam Riometers

## HAARP riometer data.

An example of these data is shown in in the left figure below. The diagram presents the riometer recordings for an interval of 1.5 days. The riometer data are displayed in blue line, the quiet day curve (QDC) in green, and absorption in red line. Note the spiky absorption event up to ~2 dB



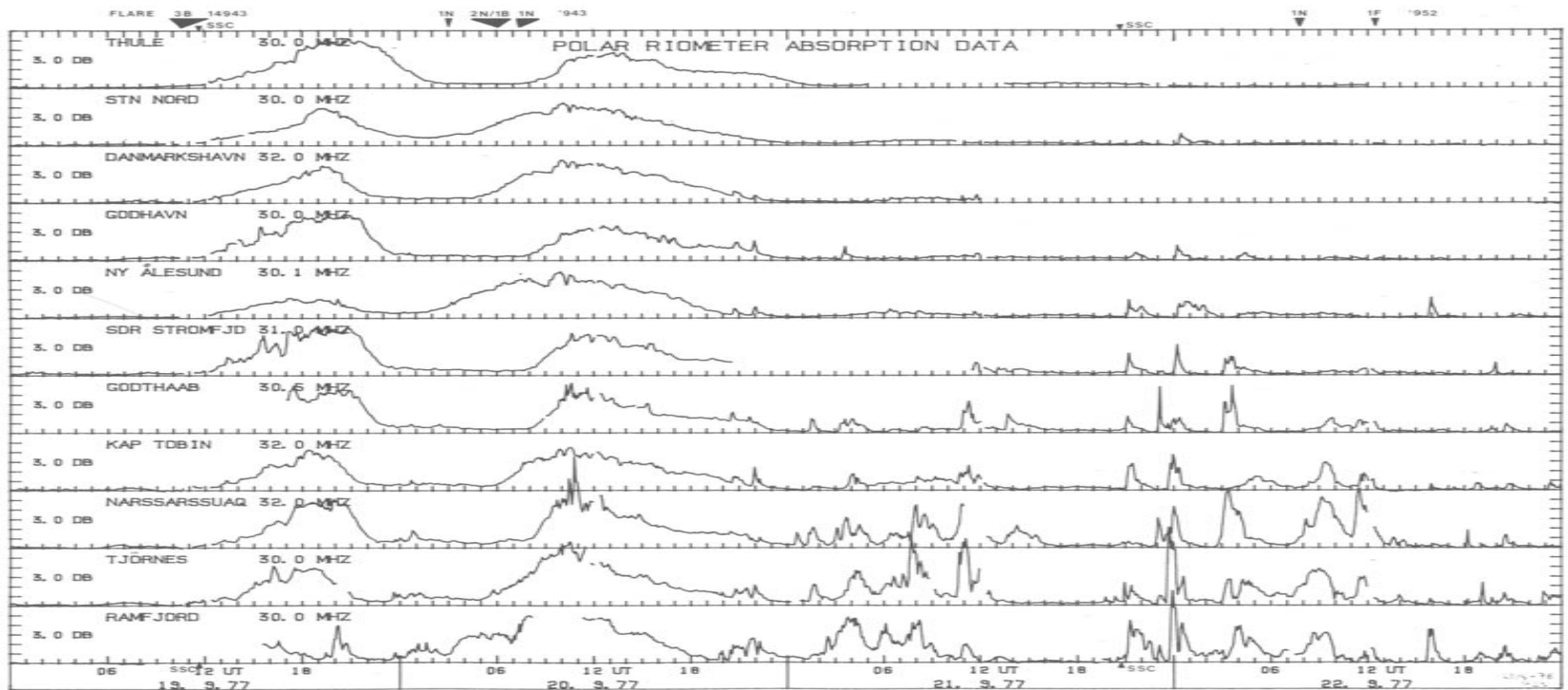
The riometer data from the HAARP installation are available on-line in real time from the link: (<http://www.haarp.alaska.edu/haarp/data.htm>). The right figure below displays the on-line real-time data from 3 consecutive days. Note the series of auroral absorption events recorded on the last day (10 Oct 2010) of the recorded interval. At other times (mostly around local noon) the recordings are disturbed by interference that generates spiky positive (upward) deflections.



[<http://www.haarp.alaska.edu/haarp/data.html> ]

# Riometers

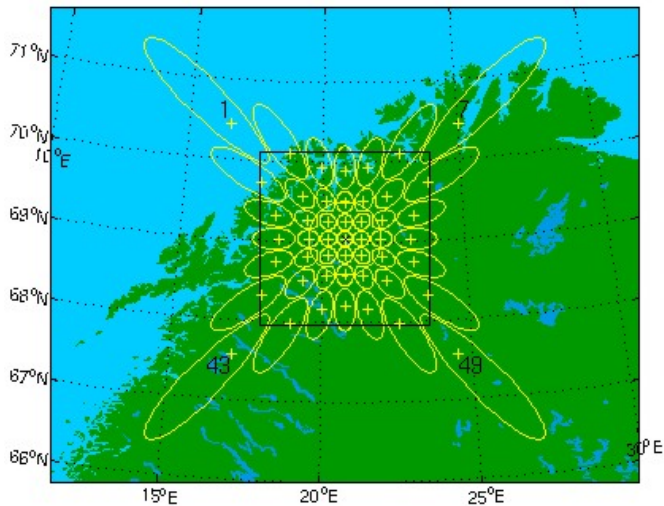
The figure displays riometer data during a major solar flare event. The black triangles mark the occurrences of major flares. The absorption intensities increase at all latitudes from auroral (bottom) to polar cap (top) to form a Polar Cap Absorption (PCA) event just after the flare events as the result of the intense radiation of high-energy solar protons, typically 10 – 100 MeV, that may reach down to the lower part of the ionospheric D-region at altitudes around 60-90 km. The PCA absorption relate to the solar proton flux as:  $L \text{ [dB]} \sim 0.13 F^{1/2} \text{ [p>20MeV cm}^{-2} \text{ s}^{-1}]$



[Stauning, 1978]

# Imaging Riometers

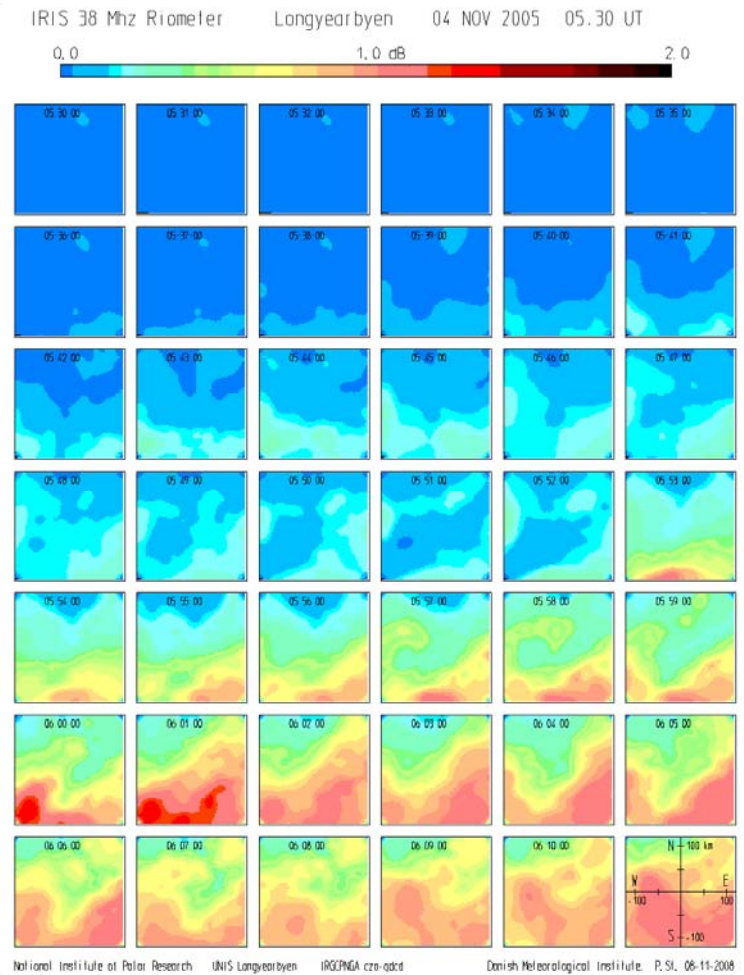
Absorption events could be studied in greater details by imaging riometers. The figure below displays the multiple antenna beam patterns for the IRIS installation at Kilpisjärvi in Northern Finland.



<http://www.dcs.lancs.ac.uk/iono/iris>

Absorption intensities derived from the 49 discrete beams can be processed to provide a continuous 2-D map of absorption intensities with dimensions of around 250 x 250 km. Such images can then be stacked to provide an overview of the time-history of absorption events.

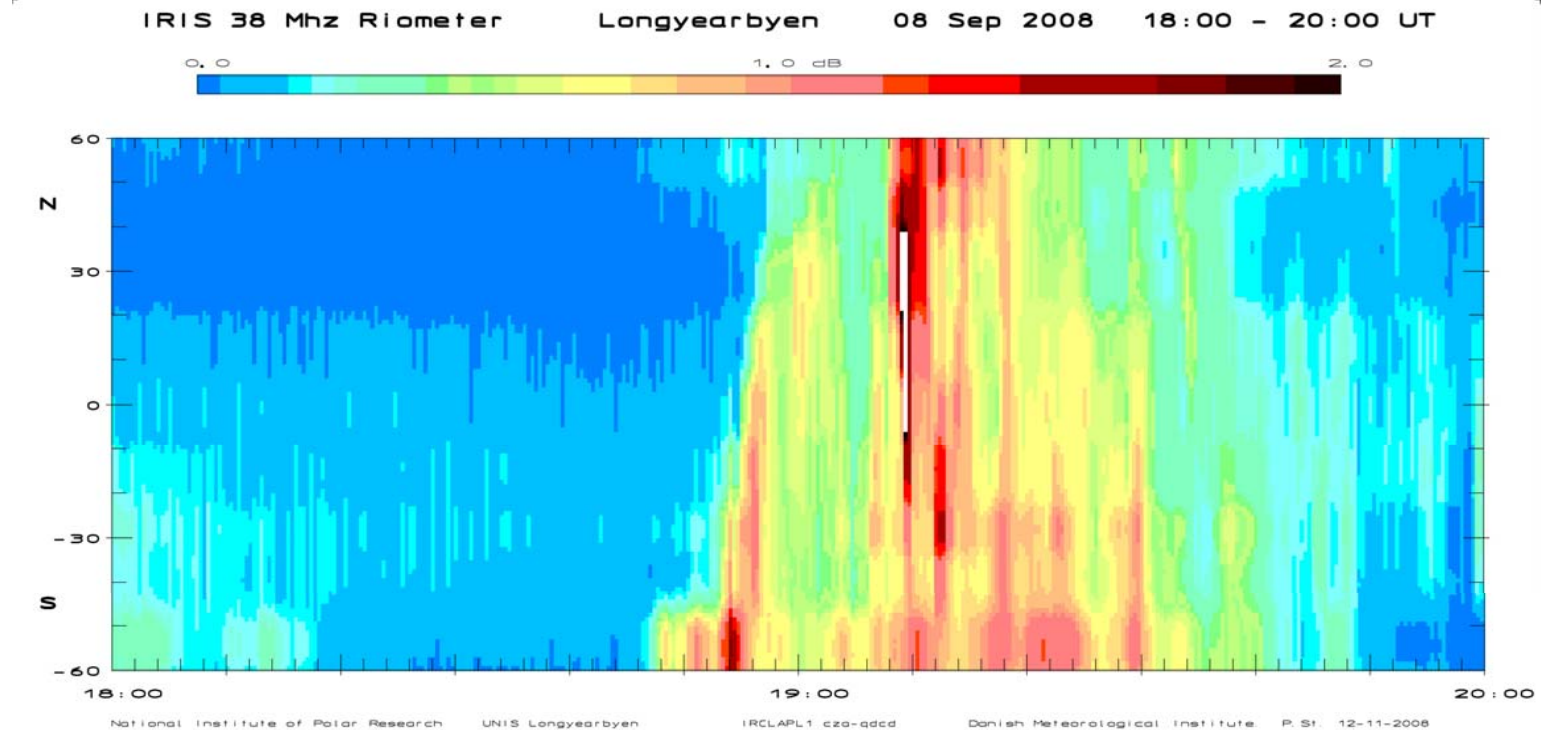
## Stacked 2-D riometer absorption maps



[Stauning, 2006]

# Imaging Riometers

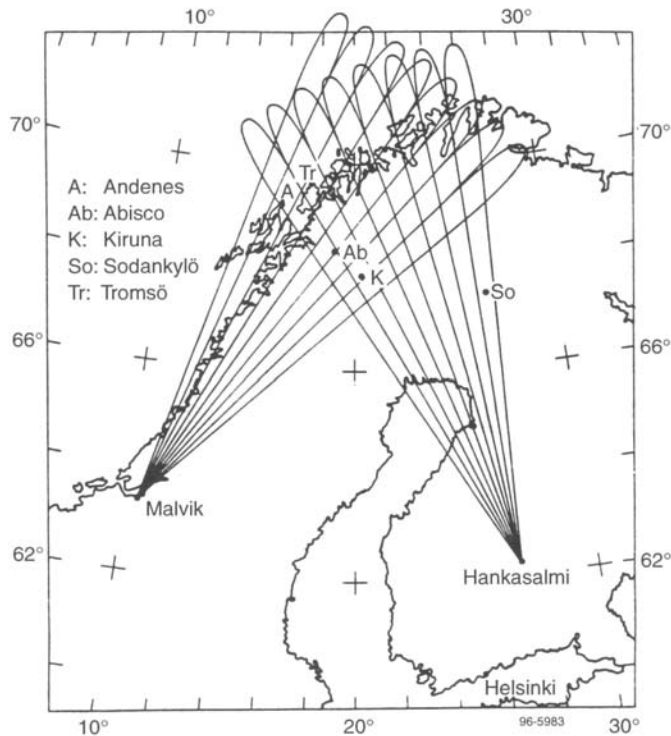
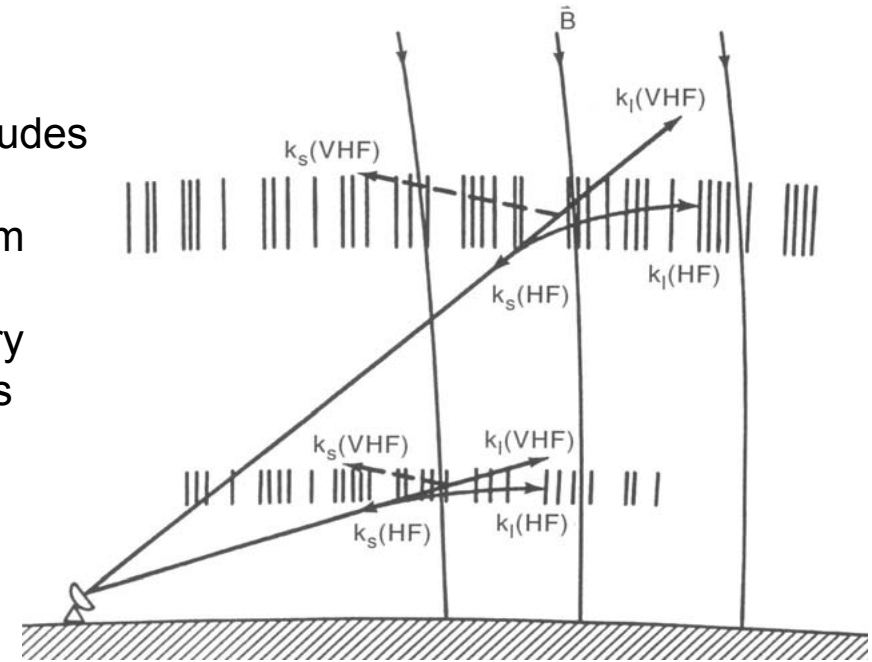
IRIS data can also be displayed in latitude-time diagrams as shown below. Here, the display extends 100 km north and south of the station. Each vertical strip in the diagram represents a N-S section of the instantaneous absorption image. The strips from a sequence of images are then stacked to provide a continuous time history of the latitudinal development. Note here that the region of enhanced absorption starts in the south and then expands poleward to reach somewhat north of the field-of-view. Thereafter the absorption region retreats equatorward.



[Stauning, 2006]

# Coherent Scatter Radars

The ionospheric irregularities that provide the backscatter of VHF signals are elongated in the direction of the magnetic field, which at high latitudes is nearly vertical. In order to receive a strong backscatter signal the direction of the radar beam should be such that the ray would intersect the ionospheric region perpendicular to the stationary magnetic field. Hence some bending of the ray is required in particular for F-region backscatter.



The first radar system to be operated along these lines was the “Twin Auroral Radar Experiment”, STARE, (e.g., Greenwald et al., 1978). The STARE radar system consisted of a pair of bistatic very high frequency (VHF) radars located at Malvik in Norway and Hankasalmi in Finland, respectively, operated at frequencies in the 140-160 MHz band and having a common viewing area centred over northern Scandinavia.

[Greenwald (1996), in Kohl et al., pp.394, 402]

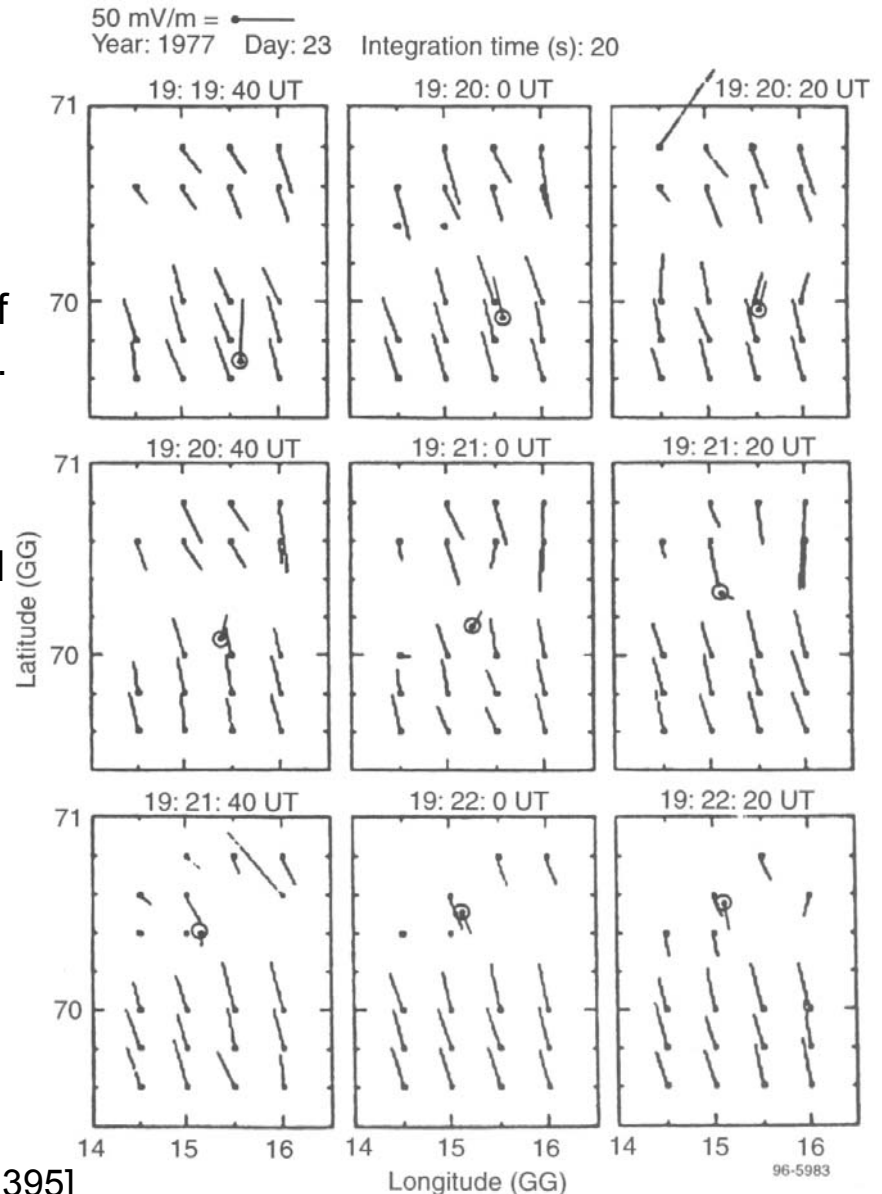
# Coherent Scatter Radars

In brief, the examination of the spectra of the backscattered signals shall provide the width of the spectrum that is controlled by the plasma temperatures, and the displacement from the centre frequency (i.e., the Doppler shift), which measures the line-of-sight convection velocity of the irregularities that provide the backscattering.

By using the pair of line-of-sight velocities the direction and magnitude of the ionospheric convection velocity can be derived over the field extended by the crossed radar beams.

The electric field vectors derived from the plasma drift have been compared to values derived from rocket-borne in-situ probe measurements. Here the STARE electric field vectors have been plotted over a section of the field-of-view that also comprises the electric field vector derived from the probe added as a bar extending from the rocket position marked by a small circle. The agreement is fair.

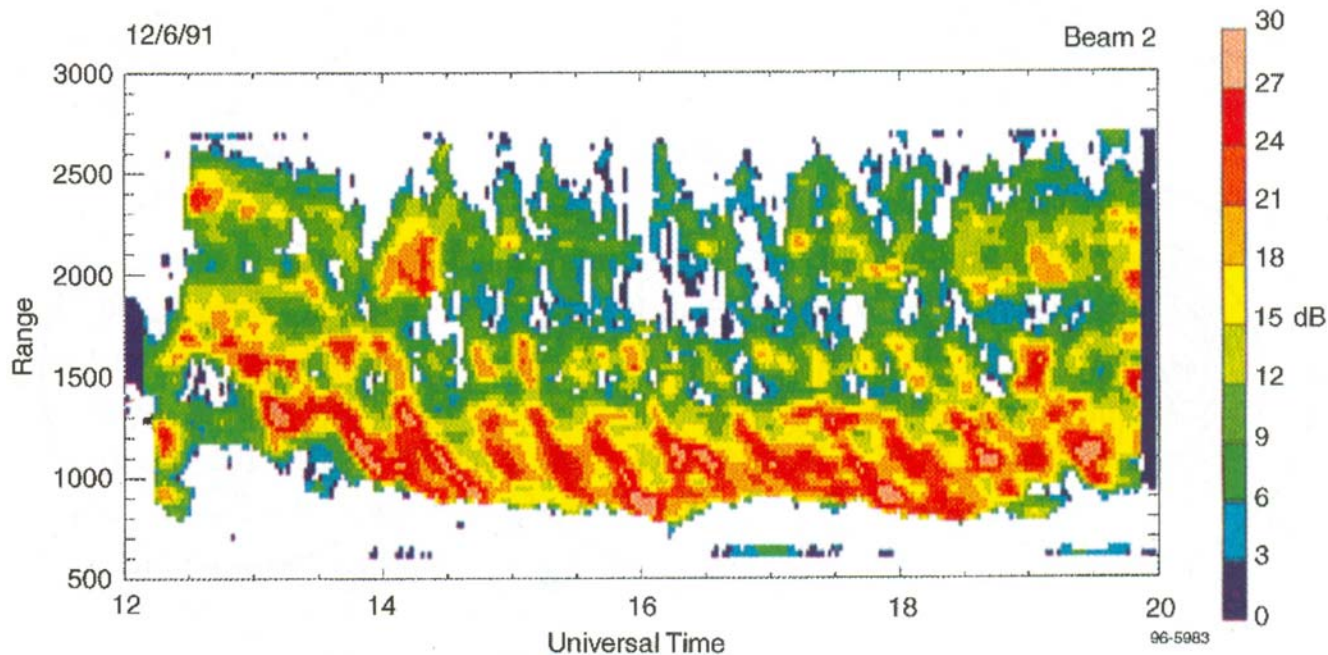
[Greenwald (1996), in Kohl et al., p.395]



# Coherent Scatter Radars, SuperDARN

A global Dual Auroral Radar Network, the SuperDARN, has been established as an international radar network for studying the upper atmosphere and ionosphere. Presently, the SuperDARN system comprises eleven radars in the northern hemisphere and seven in the southern hemisphere.

An example of the data from a single radar beam is shown below. The equatorward moving enhancements in backscatter intensity are caused by atmospheric gravity waves. [From Bristow and Greenwald, 1995, in Kohl et al. (1996), p.405].



# Coherent Scatter Radars, SuperDARN

From the received radio signals for a single radar, a number of parameters can be investigated, such as:

- line-of-sight neutral wind speeds in the mesosphere (~94 km)
- line-of-sight plasma drift speeds in the ionosphere (~100 km and 400 km altitude)
- speed, direction and wavelength of gravity waves in the ionosphere
- travelling ionospheric disturbances
- polar mesosphere summer echo occurrence (related to polar mesosphere/noctilucent clouds)
- meteor occurrence and altitude
- speed, direction and wavelength of ultra-low frequency magnetohydrodynamic waves
- space weather diagnostics (magnetic reconnection rate, magnetic field-aligned current)
- sea state

By combining such measurements from more than one radar, these phenomena may be measured across a wider range of scales, allowing estimation of:

- complete global convection in the ionosphere
- atmospheric tides and planetary waves

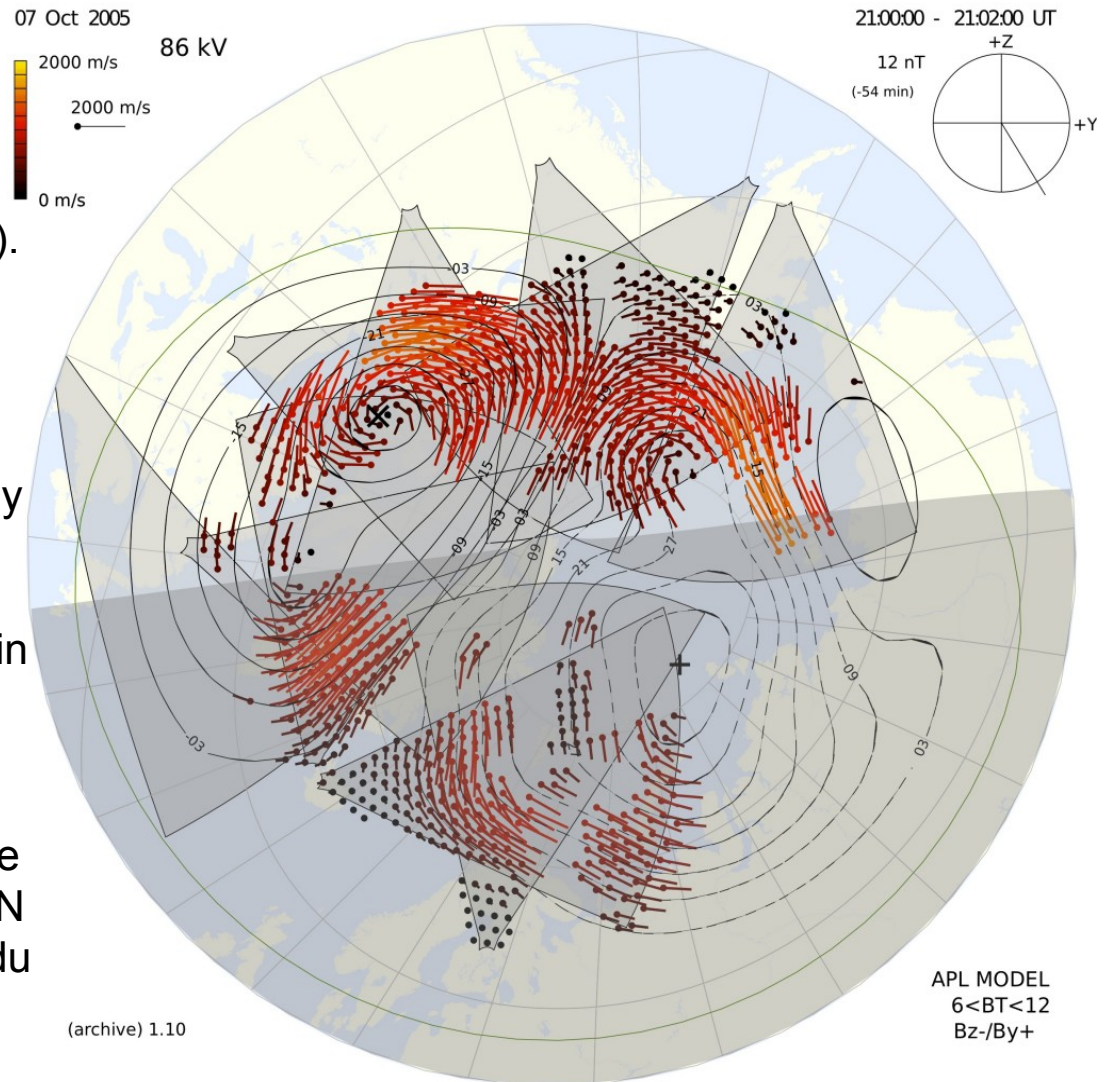
# Coherent Scatter Radars, SuperDARN

An example of global convection estimate is shown in the figure.  
(from UK SuperDARN web site:  
<http://ion.le.ac.uk/cutlass/superdarn.html> ).

The recorded convection velocities are inserted in a map of the polar electric potential structure constructed from a model assisted by the data.

The SuperDARN data are available in real time for associates of the SuperDARN community.

Information on possible access to the data are provided on the SuperDARN web page: <http://superdarn.jhuapl.edu>



# Coherent Scatter Radars, SuperDARN

The photos display the most recent addition to the SuperDARN network provided by Virginia Tech. University.

SuperDARN at Virginia Tech:  
[<http://www.space.vt.edu/superdarn> ]



# Concluding Remarks

When data from ground-based observations are used for Space Weather services, it is important to recall the properties of the observing instruments and the characteristics of their operation. Furthermore, it is important to observe the local conditions such as location in a geophysical sense (e.g., geomagnetic latitude), local time, season of the year etc.

## **A possible sequence in the scanning of data could be:**

1. Check the Dst and Kp indices to see whether a magnetic storm is ongoing.
2. Check the AE and PC indices to see whether we are in a period of polar and auroral activity.
3. Look for possible solar flare effects (from enhanced solar UV- and X-ray radiation and radio noise) like crockets in magnetograms, excessive noise mixed with impulsive absorption events in riometer recordings. Such signatures at the dayside of the Earth and preferably at middle and low geomagnetic latitudes (away from the auroral as well as the equatorial electrojets and auroral precipitation events) may signal the actual occurrence of a solar outburst.
4. Look for PCA events in riometer recordings and blackouts in ionosonde-digisonde recordings that could signal an ongoing intense solar proton event, which may start in the initial phase (within 15 min - 1 hour) of a solar outburst.

# Concluding Remarks

5. Look for signatures of Sudden Storm Commencement (SSC) in the horizontal component in mid-latitude magnetograms. SSC's are impulsive spikes that are strongest and positive at mid-day. They signal the arrival of the front of a CME cloud and may be some minutes ahead of the arrival of main bulk of CME ejecta.
6. Look around to real-time magnetograms from a number of on-line stations observing for disturbances and remembering to take into account their location and local time.
7. Check riometer recordings to observe for major auroral or polar cap absorption events.
8. Check real-time ionograms from on-line digisondes (dynasondes) to observe for irregularities in layer structures (e.g., layer heights, critical frequencies, scatter, black-out).
9. Check TEC maps to check for unusual features in the distribution or magnitude of the total electron content.
10. Hang-on to magnetograms from a selected on-line array (e.g. the Scandinavian magnetometers) to be alert to possible Space Weather developments.

**Enjoy the ride !**

# References, Links and further Reading

## References:

- Super Dual Auroral Radar Network (SuperDARN, Chisham et al., (2007), A decade of Super Dual Auroral Radar Network (SuperDARN): Scientific achievements, new techniques and future directions, *Surveys of Geophysics*, 28, 33-109, doi:10.1007/s10712-007-9017-8.
- Detrick, D. L. and T. J. Rosenberg (1990), A phased-array radiowave imager for studies of cosmic noise absorption, *Radio Science*, 25, 325-338, 1990.
- Hargreaves, J. K., Auroral absorption of HF radio waves in the ionosphere: a review of results from the first decade of riometry (1969), *Proc. IEEE*, 57, 1348-1373, 1969.
- Little, C. G. and H. Leinbach (1959), The Riometer – a device for the continuous measurement of ionospheric absorption, *Proc. IRE*, vol. 47, p. 315.
- Rawer, K. (ed.), Manual on ionospheric absorption measurements, World Data Center A for Solar-Terrestrial Physics, Report UAG-57, Boulder, 1976.
- Stauning, P. (1996), High latitude D- and E-region investigations using imaging riometer observations. *J. Atmos. Terr. Phys.*, 58, 765-783,
- Stauning, P. (1996), Investigations of ionospheric radio wave absorption processes using imaging riometer techniques. *J. Atmos. Terr. Phys.*, 58, 753-764.
- Stauning, P. (1996), Ionospheric Investigations using Imaging-Riometer Observations, in: *Review of Radio Science 1993-1996*, ed.: W. R. Stone, Oxford University Press.
- UAG Reports no. 23, “URSI Handbook on Ionogram Interpretation and Reduction” and UAG report no. 50 “High Latitude Supplement” (NOAA, Boulder, CO)

# Links and further Reading

## **Links to further reading:**

Easy reading: [www.sec.noaa.gov/Education/index.html](http://www.sec.noaa.gov/Education/index.html)

General info on ionosphere: <http://www.swpc.noaa.gov/info/Iono.pdf>

General info on radiowave propagation: <http://www.swpc.noaa.gov/info/Radio.pdf>

## **Links to more information on Ionosondes and Digisondes:**

How do you read the Digisonde Ionogram Plots: <http://home.swbell.net/pjdyer/esiongrm.htm>

Variables explained - brief description of FoEs, FxEs, h'Es, etc.:

<http://ulcar.uml.edu/%7Eiag/CHARS.htm>

NOAA NGDC Overview of Vertical Sounding:

<http://www.ngdc.noaa.gov/stp/IONO/ionogram.html>

Basic Ionosonde Theory: [http://www.wdc.rl.ac.uk/ionosondes/ionosonde\\_basics.html](http://www.wdc.rl.ac.uk/ionosondes/ionosonde_basics.html)

Background to Ionospheric Sounding: <http://ulcar.uml.edu/DPS.htm>

Case Study of an Ionosonde Movie: <http://www.wdc.rl.ac.uk/ionosondes/contents.html>

## **Online Ionosonde and Digisonde real-time data :**

HAARP - Gakona, AK: <http://www.haarp.alaska.edu/haarp/data.html>

HAARP latest ionogram : <http://137.229.36.56/latestFrames.htm>

College, AK: [ftp://solar.sec.noaa.gov/pub/lists/iono\\_day/College\\_iono.txt](ftp://solar.sec.noaa.gov/pub/lists/iono_day/College_iono.txt)

Haystack, MA: <http://digisonde.haystack.edu/>

Ionosonde, Tromsø Geophysical Observatory (TGO): <http://geo.phys.uit.no/ionosonde/>

Italy - Rome : <http://dps-roma.ingrm.it/>

United Kingdom - Fairford AFB [ftp://solar.sec.noaa.gov/pub/lists/iono\\_day/Fairford\\_iono.txt](ftp://solar.sec.noaa.gov/pub/lists/iono_day/Fairford_iono.txt)

# Links and further Reading

## **TEC and scintillation data:**

Total electron content: [http://iono.jpl.nasa.gov/latest\\_rti\\_global.html](http://iono.jpl.nasa.gov/latest_rti_global.html)

Northwest Research Associates (NWRA): [http://www.nwra.com/ionoscint/sp\\_intro.html](http://www.nwra.com/ionoscint/sp_intro.html)

Scintillation levels at solar max: [http://www.nwra.com/ionoscint/sp\\_solmax.html](http://www.nwra.com/ionoscint/sp_solmax.html)

NWRA real-time data: [http://www.nwra.com/ionoscint/sp\\_rtdata.html](http://www.nwra.com/ionoscint/sp_rtdata.html)

## **Riometer information and data:**

Description: <http://www.haarp.alaska.edu/haarp/Rio.htm>

Riometer system: <http://www.lajollasciences.com>

Global riometer locations and data: <http://www.dcs.lancs.ac.uk/iono/gloria>

On-line data : <http://www.haarp.alaska.edu/haarp/data.htm>

Imaging riometer: <http://www.dcs.lancs.ac.uk/iono/iris>

## **SuperDARN information and data:**

SuperDARN Network at Johns Hopkins Applied Physics Laboratory

<http://superdarn.jhuapl.edu/>

SuperDARN at the University of Alaska Geophysical Institute : <http://superdarn.gi.alaska.edu>

SuperDARN at Virginia Tech: <http://www.space.vt.edu/superdarn>

UK SuperDARN: <http://ion.le.ac.uk/cutlass/superdarn.html>

Super Dual Auroral Radar Network (SuperDARN real-time data (need registration and password): <http://superdarn.jhuapl.edu/archive/cnvmap.north.html>

After registration: <http://superdarn.jhuapl.edu/cgi-bin/validate.cgi>

# References

## **Models:**

All models: [nssdc.gsfc.nasa.gov/space/model/models\\_home.html](http://nssdc.gsfc.nasa.gov/space/model/models_home.html)

## **Advanced reading:**

Brekke, A: Physics of the Upper Polar Atmosphere, Wiley, 1997

Davies, K.: Ionospheric Radio, P. Peregrinus, London, 1990

Hargreaves, J.K.: The Solar-Terrestrial Environment, Cambridge Atmospheric and Space Science Series, 1992

Asgeir Brekke: Physics of the Upper Polar Atmosphere, Wiley, 1997

Handbook of Geophysics and Space Environment, AFGRL, 1985

Kohl, H., R. Rüster, and K. Schlegel (eds.), Modern Ionospheric Science, European Geophysical Society, FRG 1996.